Proceedings World Geothermal Congress 2000
Kyushu - Tohoku, Japan, May 28 - June 10, 2000

NATURAL STATE SIMULATION OF THE KAKKONDA GEOTHERMAL FIELD, JAPAN

Yukihiro Sakagawa[1], Kengo Aoyama[2], Ken Ikeuchi[1], Masahiro Takahashi[2], Osamu Kato[1], Nobuo Doi[1], Toshiyuki Tosha[3], Takao Ominato[3] and Kazuo Koide[3]

[1]Japan Metals and Chemicals Co., Ltd., 72-2 Sasamori, Ukai, Takizawa-mura, Iwate 020-0172, Japan

[2]JMC Geothermal Engineering Co., Ltd., 72-2 Sasamori, Ukai, Takizawa-mura, Iwate 020-0172, Japan

[3]New Energy and Industrial Technology Development Organization, 3-1-1 Higashiikebukuro Toshima-ku, Tokyo 170-6028, Japan

Key Words: geothermal, natural state simulation, Kakkonda field, NEDO's project

ABSTRACT

A numerical study of the Kakkonda field which consisted of three-dimensional natural state simulation, history matching and future prediction, is being carried out. Among them, the natural state simulation with porous models is presented here. Satisfactory fits on temperature in the natural state were obtained. The result implies that the heat source at the depth drives the fluid which originates from the meteoric water to form the current hydrothermal system, and that the temperature gap between the deep reservoir and the shallow reservoir may be caused by the permeability difference between both reservoirs. A sketch of the geological structure, the outline of the numerical model and results of the natural state simulation are presented.

1. INTRODUCTION

New Energy and Industrial Technology Development Organization (NEDO) started the "Deep Seated Geothermal Resources Survey" project in 1992 (Sasada *et al*., 1993). This study is being carried out as a part of the project in order to develop a proper numerical model taking into account the results of surveys of the project, and to find out the best way to develop the deep seated geothermal resources.

The Kakkonda geothermal field, located in northeastern Honshu, Japan (Figure 1), was studied by the Geological Survey of Japan (GSJ) from 1958. Japan Metals & Chemicals Co., Ltd. (JMC) investigated the geothermal system and drilled several wells to assess its potential for electric power generation. JMC currently provides steam to power station Unit 1 (50 MWe), operated since 1978, and Tohoku Geothermal Energy Co., Ltd. (TGE) provides steam to Unit 2 (30 MWe), operated since 1996.

The Kakkonda field is a liquid-dominated field, hosted by a complex sequence of sedimentary and volcanic rocks, ranging in age from pre-Tertiary to Quaternary (Nakamura and Sumi, 1981; Sato, 1982; Kato and Doi, 1993; Kato *et al*., 1993; Doi *et al*., 1995). These rocks have been intruded by the Tertiary tonalite, the Matsuzawa dacite, the 4.9±0.1 Ma Torigoeno-taki dacite (Tamanyu, 1980), and the 0.07–0.34 Ma Kakkonda granite (Kanisawa *et al*., 1994). Pre-Tertiary formations consist of slate, sandstone and andesitic tuff. Miocene formations in this sequence, andesitic tuff, dacitic tuff, shale and siltstone, are divided into the Obonai, the Kunimitoge, the Takinoue-onsen and the Yamatsuda Formations, in order of decreasing age. The Tamagawa Welded Tuffs, Pliocene to Pleistocene in age, consist of dacitic tuff and andesitic tuff. The Kakkonda granite, which has been encountered in the field at depths below 1140-2840 m, has metamorphosed formations below the Kunimitoge Formation, with extensive development of biotite, cordierite, anthophyllite, orthopyroxene, andalusite, spinel, magnetite, K-feldspar, and other metamorphic minerals (Kato and Doi, 1993; Doi *et al*., 1998).

The Kakkonda hydrothermal system consists of a shallow and a deep reservoir, which are hydraulically connected but otherwise have different characteristics (Hanano, 1995). The boundary between them is indicated by rapid increases in borehole temperatures at depths of around 1,500 m (MD). The shallow reservoir, which is characterized by a slightly alkaline fluid (at atmospheric pressure and room temperature), has a temperature of 230–260°C and is elongated in a NW direction (Figure 1). In contrast, the deep reservoir is characterized by pH of 3.2–4.5 (at atmospheric pressure and room temperature), has temperature greater than 300°°C, and is less permeable (e.g. Hanano, 1995; Yanagiya *et al*., 1996). Permeable fractures in the deep reservoir are located mainly within and at the margin of the Kakkonda granite, as well as in surrounding metamorphic rocks (Kato and Sato, 1995). Underlying the deep reservoir is a zone of conductive heat transfer, the presence of which is indicated by an abrupt change in thermal gradient within the Kakkonda granite at the depth of around 3,100 m (MD) in WD-1a (Ikeuchi *et al*., 1998). The Kakkonda granite is regarded as a part of the heat source to the hydrothermal system (Kato and Doi, 1993).

The origin of the fluid in both the shallow and deep reservoirs seems to be meteoric water (Kasai *et al*.,1998). But in the Kakkonda field, there are no wells where the temperature distribution in them indicates down flux in the reservoir. Hence, there seems to be a recharge area of meteoric water outside the well field.

In this study, three-dimensional natural state modelling was carried out with porous models. This study proceeded aiming at good matches for the temperature distribution of the natural state. In this study we used FIGS3C which is a simulator jointly developed by JMC Geothermal Engineering Co., Ltd. and Technical Software & Engineering Inc. This simulator is capable of analyzing three-dimensional transient mass and heat transport in porous or fractured media up to 1,000°C and 1,000 bars.

2. STUDY AREA AND GRID GEOMETRY

Since the shallow reservoir is elongated in a NW direction, the grids are directed to the same direction. The horizontal study area is 17.2 km along SE-NW and 13.2 km along SW-NE, and is divided into 32x21 grids (Figure 2). This area covers the Kakkonda field and the mountainous area around the field, since the mountain ridges are thought to be the limit of the natural fluid convection.

The study area is 4,600 m thick in the vertical direction, from

600 m (ASL) which is slightly lower than the ground surface of the Kakkonda field, to –4,000 m (ASL) which is sufficiently deeper than the well bottom of WD-1a (Figure 3). The study area is divided into 27 layers.

3. ROCK PROPERTIES

The values of rock density, heat capacity and thermal conductivity imposed to the numerical model are homogeneous, and are 2,500 kg/m^3, 1,000 J/(kg·K) and 2.3 W/(m·K) respectively. The porosity is set homogeneous in each layer, and decreases with depth from 18.3% in the top layer to 8.5% in the bottom layer. The values of porosity are decided based on the sonic and density log results of WD-1 series and on the analysis result of the electric logs of other wells.

With respect to permeability, the study area is divided to a few domains, such as the shallow reservoir, the deep reservoir, the margin of the Kakkonda granite, northeastern area far from the well field, and so on. Permeability is anisotropic in this study. The values of permeability are constrained to some extent by the analysis result of temperature distribution using one-dimensional vertical-ascending flow model (Kajiwara *et al*.,1993), the analysis result of permeability values, and the anisotropy from pressure monitoring done as a part of the NEDO's project. One of the vertical sections of the z-direction permeability distribution is shown in Figure 4 as an example.

4. BOUNDARY AND INITIAL CONDITIONS

The top boundary is open with respect to mass and heat flow. To permit the fluid flow we imposed a pressure distribution to the boundary surface. The pressure distribution is set heterogeneous; the area where the ground surface is relatively high has a relatively high boundary pressure. The mountainous area surrounding the Kakkonda field might be the recharge zone of the meteoric water to the field. The elevation of the ground surface at each grid is read and shown in Figure 5. To permit the conductive heat flow we imposed a temperature distribution to the boundary surface. The temperature distribution is set homogeneous at the value of 20°C.

With respect to the bottom boundary, a temperature distribution is imposed to permit the conductive heat flow which makes all the heat source to the field. The temperature distribution at the bottom surface (Figure 6) is decided on basis of the temperatures in wells far from Kakkonda, and the temperature of the Kakkonda granite measured in WD-1a. On the other hand, the bottom surface is closed to mass flow. Since the origin of the fluid in the deep reservoir seems to be meteoric water, it is likely that there is little ascending flow in the zone of conductive heat transfer. The bottom surface is so deep, and the temperature at the depth of the bottom surface is so high, that the rock may be ductile and the fluid may not flow.

Side boundaries are closed to both conductive heat flow and mass flow. Theoretically, they are not wholly closed. However, the high pressure potential at mountains may prevent flow across them. Also, the future prediction will become conservative with the closed boundary conditions.

The initial temperature distribution is linear with depth and laterally uniform; 20°C at the top surface and the temperature gradient is 0.1°K/m. The temperature gradient is set the same as measured in a well far from Kakkonda. Since the temperature far from Kakkonda may not be affected by the current geothermal activity at the Kakkonda, it may indicate the temperature in the Kakkonda at the time before the current geothermal activity. The initial pressure is hydrostatic with the uniform pressure distribution of 1 bar at the top surface.

5. RESULT OF THE NATURAL STATE SIMULATION

The calculation is made to achieve a steady state. In this study, the natural state is regarded as a steady state, since the geothermal evolution history is not very clear. With respect to the best model, the duration of the calculation is 300,000 years.

5.1 The Temperature Fits

The result of the natural state simulation is fitted to temperature distributions in wells which indicate temperatures in the natural state. Figure 7 shows some of the temperature fits for the best model. The calculated temperatures in Figure 7 are the temperatures of the grids which the wells penetrate, and the minimum and maximum temperatures in laterally neighboring grids. The figure shows good fits in general. Especially the temperature gap between the shallow reservoir and the deep reservoir is clearly reproduced for Well-18. Also, the temperature gradient in the deep conductive zone in the Kakkonda granite is reproduced for WD-1a.

The two-layered temperature structure in which the deep reservoir has higher temperature than the shallow reservoir, may be caused by the permeability difference between both reservoirs (Hanano, 1998). The mechanism, where the two-layered permeability structure might result in the two-layered temperature structure, may be as follows: Since the permeability in the shallow reservoir is high compared with the deep reservoir, the fluid in the shallow reservoir flows more vigorously than in the deep reservoir so that the temperature in the shallow reservoir becomes rather uniform at the temperature between the atmospheric temperature and the temperature in the deep reservoir. If we stand in the deep reservoir, we will see that the temperature of the upper boundary, which is the boundary between both reservoirs, is kept lower. When the hot water ascends to the constant temperature boundary at steady state, the temperature of the water is almost uniform in the depth because the cool boundary is too far to affect the temperature. On the other hand, the nearer the water ascends to the boundary, the stronger the effect of the boundary becomes, and the water becomes cooler. That is how the temperature changes abruptly near the boundary of both reservoirs to make the two-layered temperature structure.

5.2 Temperature distribution and meteoric recharge distribution

Figure 8 shows the calculated temperature distribution in a section. This figure shows the conductive zone below the deep reservoir, relatively homogeneous zones of the shallow reservoir and the deep reservoir, and the steep temperature gradient between both reservoirs.

Figure 9 shows the calculated meteoric recharge distribution. This figure shows a wide recharge zone surrounding the Kakkonda field. The recharge zone seems to be slightly nearer to

the Kakkonda field than the mountain ridge which can be discerned in Figure 5.

6. HYDROTHERMAL SYSTEM OF THE KAKKONDA FIELD

In this study, it is confirmed that the temperature distribution in the hydrothermal system of the Kakkonda field can be generated by the combination of a heat source at depth, and the meteoric water recharge. This means that the mass source from the great depth may not exist, or contributes little to the convection zone above or the deep reservoir. This concept is consistent with the geochemistry which implies that the origin of the fluid in the shallow and deep reservoirs seems to be meteoric water.

7. CONCLUSIONS

The numerical model constructed in this study was shown to reproduce the temperature distribution in wells in the natural state. Therefore we can say that our conceptual model is feasible. This means that the heat source at the depth drives the fluid which originates from the meteoric water to form the current hydrothermal system of the Kakkonda field without much contribution of the magmatic recharge. Also, the fact that two-layered temperature structure in which the deep reservoir, has higher temperature than the shallow reservoir, may be caused by the permeability difference between the reservoirs. We estimate from this study that the wide area surrounding the Kakkonda field seems to be the zone of the meteoric recharge to the reservoir.

ACKNOWLEDGMENTS

The authors wish to thank Dr. Mineyuki Hanano of JMC for his helpful suggestions to the study, and NEDO, JMC and TGE for their permission to publish this paper. The authors would like to thank the anonymous referee for helpful suggestions.

REFERENCES

Doi, N., Kato, O., Kanisawa, S. and Ishikawa, K. (1995). Neo-techtonic fracturing after emplacement of Quaternary granitic pluton in the Kakkonda geothermal field, Japan. *Geothermal Resources Council Trans*. **19**, pp.297-303.

Doi, N., Kato, O., Ikeuchi, K., Komatsu, R., Miyazaki, S., Akaku, K. and Uchida, T. (1998). Genesis of the plutonic-hydrothermal system around Quaternary granite in the Kakkonda geothermal system, Japan. *Geothermics* **27**, pp.663-690.

Hanano, M. (1995). Hydrothermal convection system of the Kakkonda geothermal field, Japan. *Proc. World Geothermal Congress '95*, Florence, Italy, pp.1629-1634.

Hanano, M. (1998). A simple model of a two-layered high-temperature liquid-dominated geothermal reservoir as a part of a large-scale hydrothermal convection system. In: *Transport in Porous Media* **33**, Kluwer Academic Publishers, Netherlands, pp.3-27.

Ikeuchi, K., Doi, N., Sakagawa, Y., Kamenosono, H. and Uchida, T. (1998). High-temperature measurements in well WD-1a and the thermal structure of the Kakkonda geothermal system, Japan. *Geothermics* **27**, pp.591-607.

Kajiwara, T., Hanano, M., Ikeuchi, K. and Sakagawa, Y. (1993). Permeability structure at the Kakkonda geothermal field, Iwate Prefecture, Japan. *1993 Annual Meeting, Geothermal Research Society of Japan, Abstracts and Programs*, B30. (in Japanese).

Kanisawa, S., Doi, N., Kato, O. and Ishikawa, K. (1994). Quaternary Kakkonda granite underlying the Kakkonda geothermal field, Northeast Japan. *J. Min. Petr. Econ. Geol*. **89**, pp.390-407. (in Japanese with English abstruct).

Kato, O. and Doi, N. (1993). Neo-granitic pluton and later hydrothermal alteration at the Kakkonda geothermal field, Japan. *Proc. 15th NZ Geothermal Workshop*, pp.155-161.

Kato, O., Doi, N. and Muramatsu, Y. (1993). Neo-granitic pluton and geothermal reservoir at the Kakkonda geothermal field, Iwate Prefecture, Japan. *J. Geothermal Research Society Japan* **15**, pp.41-57. (in Japanese with English abstruct).

Kato, O., Doi, N., Sakagawa, Y. and Uchida, T. (1998). Fracture systematics in and around well WD-1, Kakkonda geothermal field, Japan. *Geothermics* **27**, pp.609-629.

Kato, O. and Sato, K. (1995). Development of deep-seated geothermal reservoir bringing the Quaternary granite into focus in the Kakkonda geothermal field, Northeast Japan. *Resource Geology* **45**, pp.131-144. (in Japanese with English abstruct).

Nakamura, H. and Sumi, K. (1981). Exploration and development at Takinoue, Japan. In: *Geothermal Systems, Principles and Case Histories*, L. Rybach and L. J. P. Muffer (Ed)., John Wiley & Sons Ltd., pp.247-272.

Sasada, M., Miyazaki, S. and Saito, S. (1993). NEDO's Deep-Seated Geothermal Resources Survey at the Kakkonda System, Northeast Japan. *Geothermal Resources Council Transactions*, Vol.17, pp.181-185.

Sato, K. (1982). Analysis of geological structure in the Takinoue geothermal area. *Journal Geothermal Research Society Japan* **3**, pp.135-148.

Tamanyu, S. (1980). Radiometric dating of igneous rocks in the Sengan area. *Research on Hydrothermal Systems, Interim Report Japan's Sunshine Project*, FY1978 to 1979, Geol. Surv. Japan, pp.15-23. (in Japanese).

Uchida, T., Akaku, K., Sasaki, M., Kamenosono, H., Doi, N. and Miyazaki, S. (1996). Recent Progress of NEDO's "Deep-Seated Geothermal Resources Survey" Project. *Geothermal Resources Council Trans*. **20**, pp.643-648.

Yanagiya, S., Kasai, K., Brown, K. L. and Giggenbach, W. F. (1996). Chemical characteristics of deep geothermal fluid in the Kakkonda geothermal system, Iwate Prefecture, Japan. *Chinetsu* **33**, pp.1-18. (in Japanese with English abstruct).

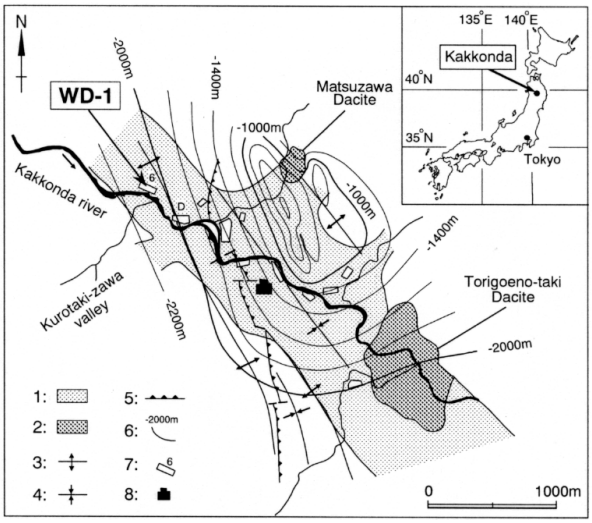

Figure 1. Schematic map of geological structure and contours of the top of the Kakkonda Granite in the Kakkonda geothermal field (after Kato et al, 1998).

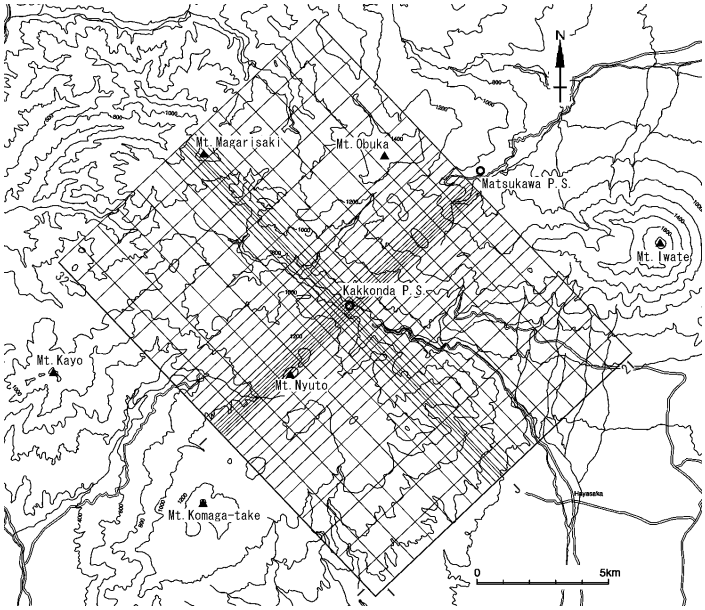

Figure 2. Horizontal study area and grid division.

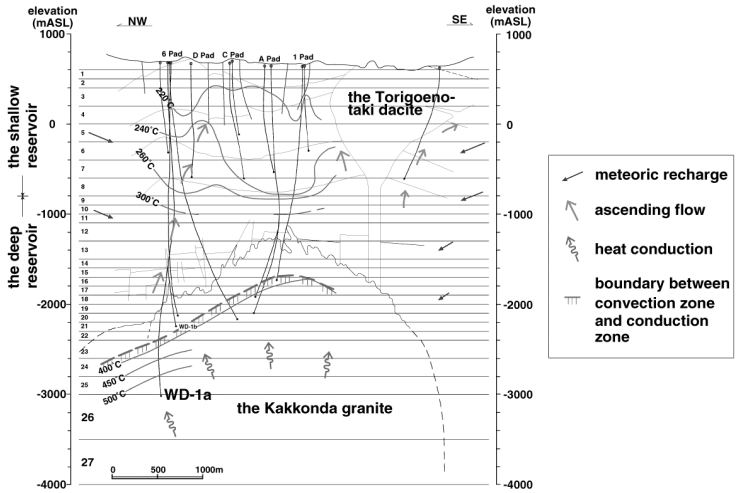

Figure 3. Vertical study area and layer division
Geological section is compiled from Uchida et al., (1996) and Ikeuchi et al., (1998).

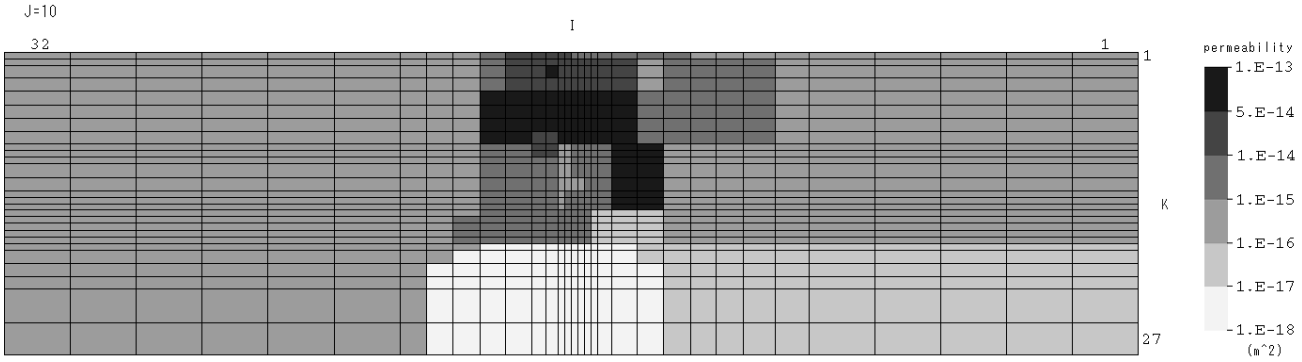

Figure 4. Permeability distribution of the best model (z-direction, vertical section at J of 10).

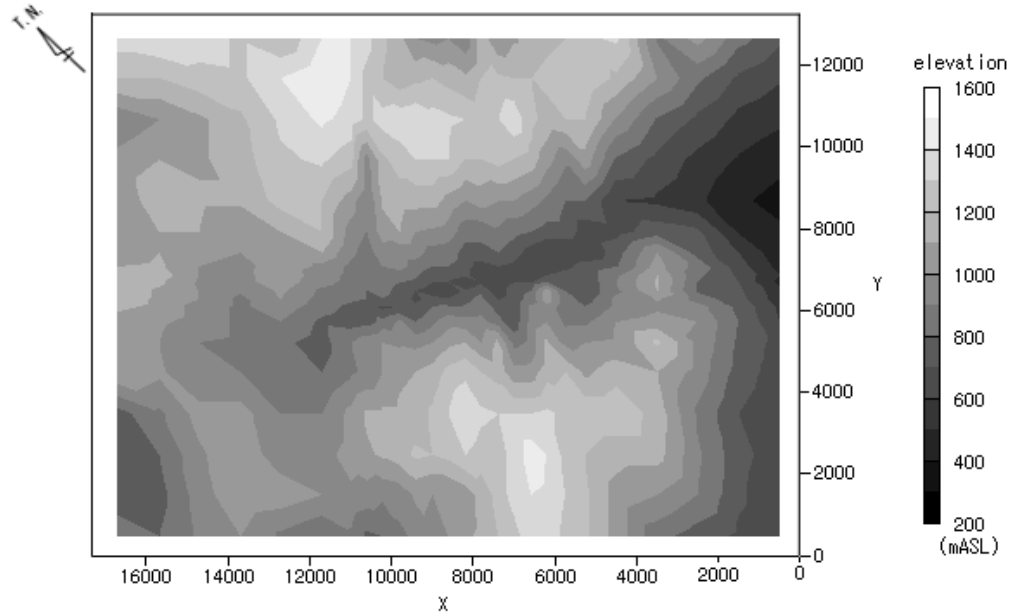

Figure 5. Topography in study area
Elevation at each grid is mapped.

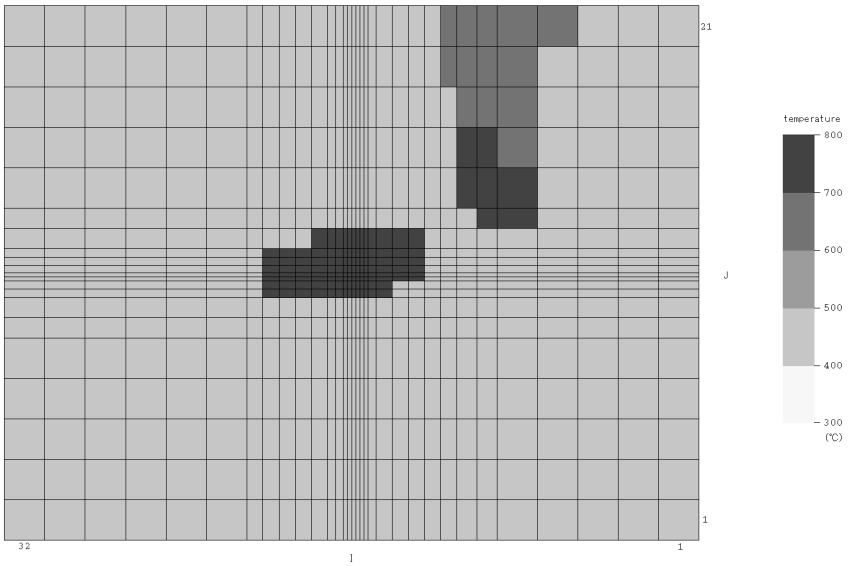

Figure 6. Temperature distribution at the bottom surface.

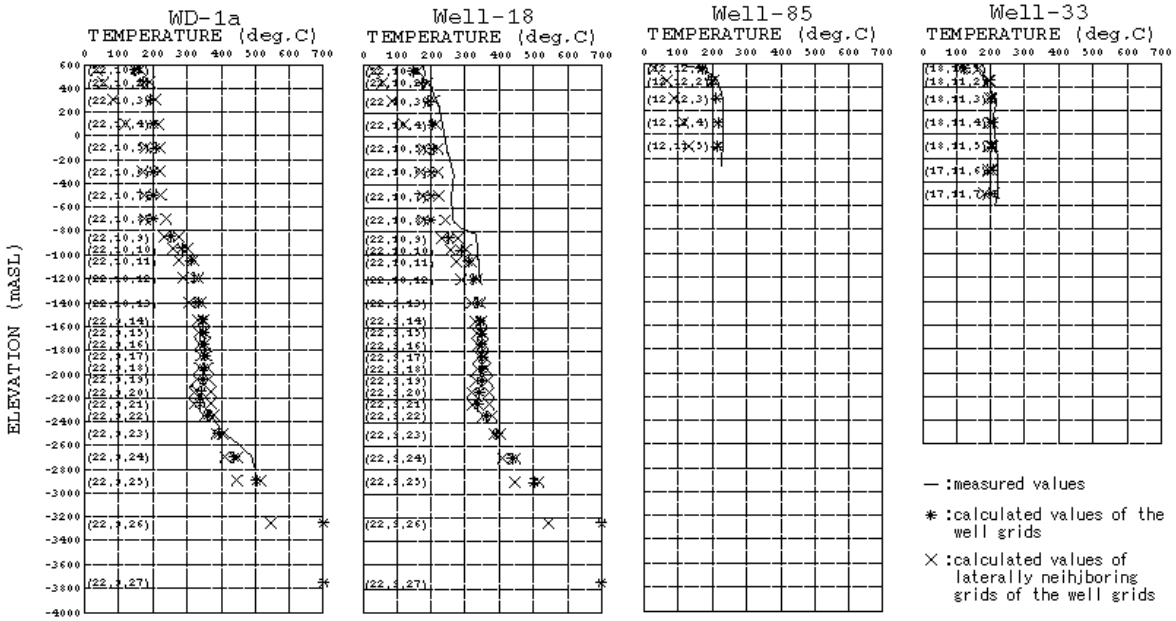

Figure 7. Some of the fits about the temparature distribution in the wells.

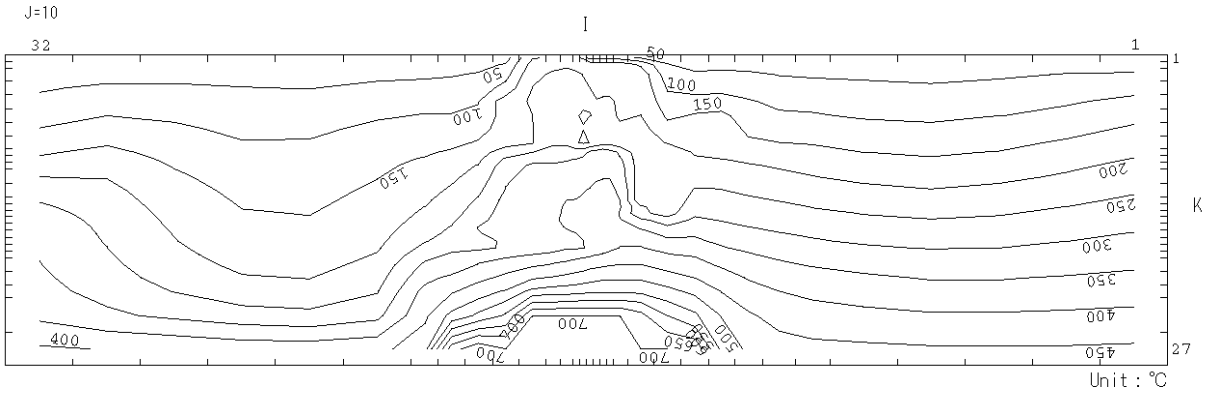

Figure 8. Calculated temperature distribution (vertical section at J of 10).

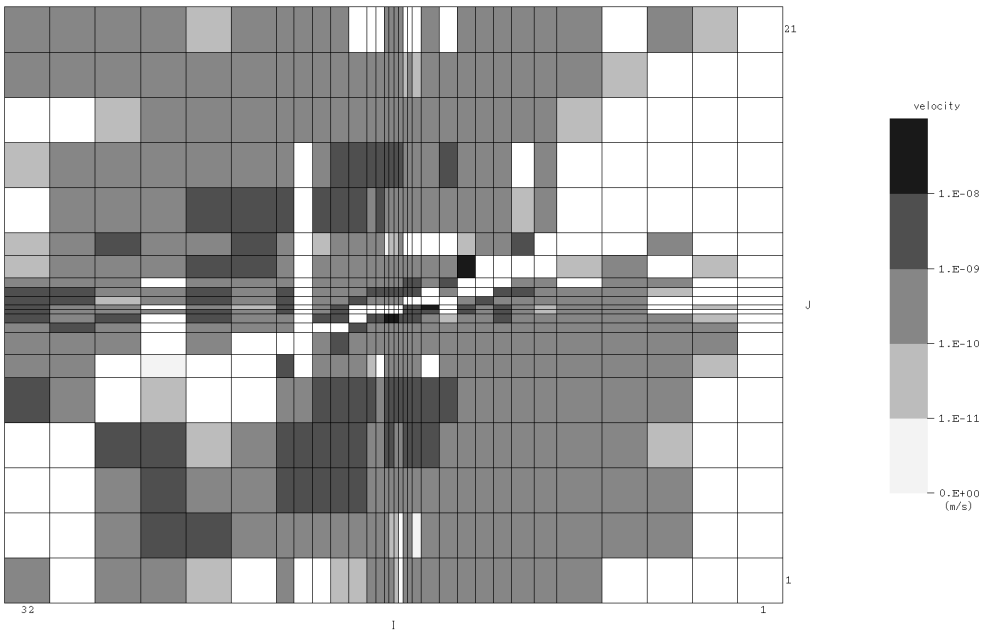

Figure 9. Calculated meteoric recharge distribution at the top boundary surface.